Performance Analysis of the Slip Power Recovery Induction Motor Drive System Under Unbalance Supply Voltages

Hilmi Fadhil AMEEN, *Fadhil Toufick AULA*

Department of Electrical Engineering, College of Engineering, Salahaddin University-Erbil, Kirkuk road, 44002 Erbil, Iraq

hilmi.ameen@su.edu.krd, fadhil.aula@su.edu.krd

DOI: 10.15598/aeee.v19i3.4050

Article history: Received Dec 16, 2020; Revised Apr 27, 2021; Accepted Jun 18, 2021; Published Sep 30, 2021.

Abstract. *This paper develops a mathematical model for analyzing the steady-state performance of the Slip Power Recovery Induction Motor Drive System (SPRIMDS) which operates under unbalance supply voltage conditions. The IEC definition indices of Voltage Unbalance Factor (VUF) and Complex Voltage Unbalance Factor (CVUF) which consist of magnitude and phase angle of the unbalance supply are used for the analysis. Also, this paper evaluates the impact of voltage unbalance and firing angle of the inverter on the stator and rotor motor parameters, motor currents, copper losses, efficiency, power factor, torque-speed characteristics, prediction of peak currents of the stator and rotor phase windings, and Total Harmonic Distortion (THD) of stator and rotor currents. The proposed mathematical model of SPRIMDS is validated using MATLAB-Simulink. The results have shown that the performance of the SPRIMDS and variation of motor currents, efficiency, THD and torque are depending on the magnitude of the voltage unbalance and inverter's firing angle.*

Keywords

Firing angle, positive and negative sequence, slip power recovery, THD, unbalance supply voltage.

1. Introduction

The majority of electrical devices is designed to operate under symmetrical and pure sinusoidal supply voltages. However, in reality, voltages and currents in an electrical power system are rarely sinusoidal and balanced. Any change in the main unbalanced supply voltage will deteriorate the characteristics of the Induction Motor (IM) [1] and [2]. In power systems, there are two reasons for producing an unbalance in the supply voltages. The first reason is structural which is due to the imbalance in the utilities of power system networks, such as alternators, transmission lines, transformers, and unbalanced capacitor banks. The second reason is functional, which is due to asymmetric voltage drop in impedances of the network caused by irregular load distribution in three-phase system, such as single-phase furnaces, induction furnaces, X-ray devices, electric welding machines, opening in a conductor in power system, short circuits, failure in the insulation of equipment, etc. Motor design variables such as stator and rotor slot designs and main quality affect the performance of electrical motors [3] and [4].

Many studies have suggested that the high efficiency of IM is more affected by voltage supply problems [5], [6] and [7]. The authors of [8], [9] and [10] have concluded that the magnitude of supply voltage and the angle of CVUF are sufficient to assess the performance of squirrel cage IM under unbalance supply voltage without considering their influences on Wound Rotor Induction Motor Drive System (WRIMDS).

Adjustable Speed Drives (ASD) are used to improve motor operation and control. However, the presence of voltage unbalance has a negative impact on ASD [11]. The presence of rectifier and inverter in the machine drive system is affected by voltage unbalance. The rectifier is affected by unbalancing voltage which then produces a rotor current unbalance that raises

the temperature of the rectifier diode and torque ripple. Compared to squirrel cage IM, WRIM has the ability to control the speed by introducing an external resistance into the rotor circuit or by recovering the rotor slip power to the supply [12]. Such a mechanism in WRIM makes it possible to keep the motor current low during starting with maintaining a high starting torque. Therefore, when repeated starting is necessary or with high inertia loads, which require a longer starting time, the WRIM can operate without overheating.

The slip power scheme is only possible with WRIM. Such a motor compared to a squirrel cage motor has several drawbacks such as high cost, heavy weight, large volume, and periodic maintenance due to the presence of brushes and slip-rings. However, controlling the WRIM through the rotor circuit allows economical drives to be obtained for varied applications, such as variable speed pumps, fan applications, mills, conveyors, cooling pumps, steel drives, paper drives, cranes, ventilations, cement factories, etc. A slip power converter is connected to the rotor windings via a slip-ring. The converter which consists of a bridge rectifier, a three-phase inverter, and a smoothing inductor provides a feedback power to the mains. This voltage can be controlled by controlling the firing angle of the inverter, which in turn controls the speed within the sub-synchronous speed range. The inverter is connected back to the AC supply via a recovery transformer to determine the required speed range.

The authors in [13], [14], [15], [16], [17] and [18] have proposed techniques to improve the power factor and reduce the total harmonic distortion, without considering the effect of unbalance supply voltage on the performance of SPRIMDS. The authors in [19] have analyzed the performance of slip power recovery under the power supply failure for a few cycles of operation without considering the influence of supply voltage unbalances. The authors in [20] have investigated the effect of voltage dip on the performance of SPRIMDS, the H∞ technique is proposed to reduce the effect of voltage dip on WRIM [21], neglecting the effect of the low quality of supply voltage and its impacts on it.

In this paper, the steady state performance of SPRIMDS under unbalance supply voltage is investigated. A mathematical model for the system is derived, and MATLAB Simulink is used to validate the model using the recommended IEEE equivalent circuit. The symmetrical component theory method is used to analyse the operation of the proposed mathematical model under unbalance supply voltage conditions and different firing angle. Different levels of unbalance voltages are applied on typical 1.8 kW, 50 Hz, 4-pole, WRIM. The proposed model of the drive system is analyzed under various voltage unbalance factors taking into consideration the effect of the phase angle of the unbalance supply voltage. The main objective of this paper is to analyze the influence of VUF on the motor currents, copper losses, efficiency, power factor and electromagnetic torque at different firing angles of the inverter.

2. Steady State Analysis of SPRIMDS under Unbalance Voltage Supply

Disturbance of positive sequence voltage, which is caused by negative and zero sequence voltage components, is considered as a voltage unbalance. Since the IMs are connected in delta and star connection without neutral, hence the zero-sequence component is neglected. Therefore, the negative sequence component becomes the main cause of voltage unbalance [22]. Accordingly, the voltage unbalance is the superposition of negative sequence voltage over positive sequence voltage. If the positive sequence component of voltage is disturbed, then its magnitude becomes less or more than the rated voltage [23].

In basic SPRIMDS, the rotor slip power is rectified by a full-bridge diode rectifier, a smoothing inductor is inserted to reduce the ripple in DC voltages, and then the slip power is converted to AC voltage at line frequency by using an inverter and recovered to the AC supply. This causes the speed to be controlled by varying the firing angle of the inverter in the sub-synchronous speed region as shown in Fig. 1. The concept of symmetrical component is applied in the performance analysis of SPRIMDS. The supply voltages under unbalance conditions are decomposed into positive and negative sequence components and per phase equivalent circuits are built for both components. The per-phase positive and negative sequence equivalent circuits of SPRIMDS under unbalance supply voltage conditions are derived based on the following assumptions for reducing the complexity:

- motor parameters are constant and do not depend on the frequency especially the rotor resistance and leakage reactance,
- commutation overlap angle of the bridge rectifier due to leakage motor reactance is neglected,
- rotational losses combined with core losses are constant and do not depend on the speed,
- power losses in the bridge rectifier and inverter are neglected, and
- rotor phase current alternates are the square pulse of 1200 duration.

Figure 2 shows both positive and negative sequence equivalent circuits in which R_s, X_s, X_r, X_m, R_r, R_d,

R_h, α, (n_m), and n_1 denote per phase stator resistance, per phase stator leakage reactance, rotor referred to stator leakage reactance, magnetizing reactance, rotor referred to stator resistance, smoothing inductor resistance, rotor harmonic resistance referred to stator side, the inverter delay firing angle, drive turn ratio, and stator to rotor turn ratio, respectively. Also, V_p, V_n, V_c and V_D are positive sequence supply voltage, negative sequence supply voltage, counter DC emf inverter voltage and the voltage drop of rectifier and inverter bridges, respectively. The positive sequence slip (s_p) and negative sequence slip (s_n) are given in Eq. (1) and Eq. (2), respectively.

$$s_p = s = \frac{\omega_s - \omega_r}{\omega_s}, \tag{1}$$

$$s_n = \frac{-\omega_s - \omega_r}{-\omega_s} = 2 - s. \tag{2}$$

The SPRIMDS like other drive systems is designed to operate under balanced supply voltages. While this system is subjected to unbalance supply voltages, it draws asymmetrical currents with positive and negative sequence currents. The positive and negative impedance of the SPRIMDS can be calculated from the equivalent circuit derived by using the Kerchief Voltage Law (KVL) in Fig. 2. Applying KVL in the circuit of Fig. 2(a), we can obtain:

$$V_p = I_{sp}(R_s + j(X_s + X_m)) - jI_{rp}X_m, \tag{3}$$

$$I_{rp}\left(R_h + \frac{R_d}{s} + j\left(X_r + X_m\right)\right) - \frac{V_{cp}}{s} - jI_{sp}X_m = 0, \tag{4}$$

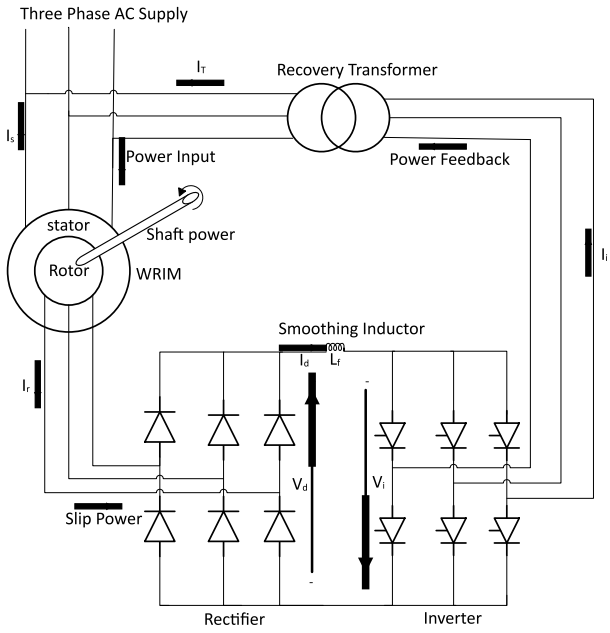

Fig. 1: Slip power recovery IM drive system.

where,

$$V_{cp} = -n_m V_p \cos\alpha + \frac{\pi n_1}{3\sqrt{6}} V_D. \tag{5}$$

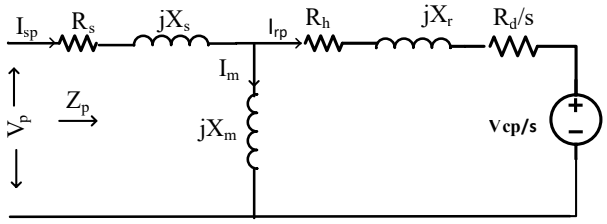

(a) Positive sequence circuit.

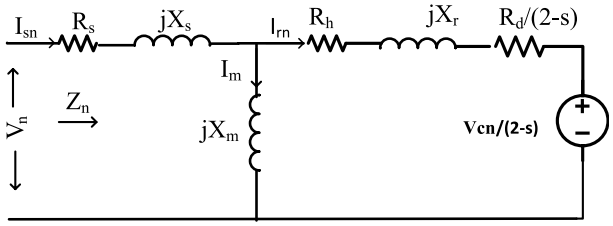

(b) Negative sequence circuit.

Fig. 2: Positive and negative equivalent circuits of SPRIMDS.

Similarly, for Fig. 2(b), we can apply KVL in two loops as,

$$V_n = I_{sn}(R_s + j(X_s + X_m)) - jX_m I_{rn}, \tag{6}$$

$$I_{rn}\left(R_h + \frac{R_d}{2-s} + j(X_r + X_m)\right) + -\frac{V_{cn}}{2-s} - jI_{sn}X_m = 0, \tag{7}$$

where,

$$V_{cn} = -n_m V_n \cos\alpha + \frac{\pi n_1}{3\sqrt{6}} V_D. \tag{8}$$

Substituting Eq. (4) into Eq. (3) and Eq. (7) into Eq. (6), and rearranging them, which are functions with slip and firing angle, the positive sequence impedance (Z_p) and negative sequence impedance (Z_n) can be obtained by using Eq. (9) and Eq. (10), respectively. The obtained Eq. (9) and Eq. (10) are functions of slip and α.

$$Z_p = \left(R_s + j(X_s + X_m) + \frac{X_m^2}{R_h + \frac{R_d}{s} + j(X_r + X_m)}\right) \cdot \left(\frac{1}{1 + j\frac{X_m n_m \cos\alpha}{sR_h + R_d + js(X_m + Xr)}}\right). \tag{9}$$

$$Z_n = \left(R_s + j(X_s + X_m) + \frac{X_m^2}{R_h + \dfrac{R_d}{2-s} + j(X_r + X_m} \right) \cdot \left(\frac{1}{(1 + j\dfrac{X_m n_m \cos\alpha}{(2-s)R_h + R_d + j(2-s)(X_m + Xr)}} \right). \tag{10}$$

Based on the equivalent circuit of SPRIMDS in Fig. 2, the positive and negative sequence rotor currents can be written as in Eq. (11) and Eq. (12) (see next page), respectively. The expression of positive sequence component, negative sequence component, and resultant of developed electromagnetic torque are obtained as in Eq. (13), Eq. (14), and Eq. (15), respectively.

$$I_{rp} = \frac{\dfrac{n_m V_p \cos\alpha}{s}\left(R_s + R_h + \dfrac{R_d}{s}\right)}{\left(R_s + R_h + \frac{R_d}{s}\right)^2 + (X_s + X_r)^2} + \frac{\sqrt{\dfrac{(n_m V_p \cos\alpha\ )^2}{s^2}\left(R_s + \ R_h + \dfrac{R_d}{s}\right)^2 + \left(\left(R_s + R_h + \dfrac{R_d}{s}\right)^2 + (X_s + X_r)^2\right)\left(V_p^2 - \dfrac{(n_m\ V_p \cos\alpha)^2}{s^2}\right)}}{\left(R_s + R_h + \frac{R_d}{s}\right)^2 + (X_s + X_r)^2}. \tag{11}$$

$$I_{rn} = \frac{\dfrac{n_m V_n \cos\alpha}{2-s}\left(R_s + R_h + \dfrac{R_d}{2-s}\right)}{\left(R_s + R_h + \frac{R_d}{2-s}\right)^2 + (X_s + X_r)^2} + \frac{\sqrt{\dfrac{(n_m V_n \cos\alpha)^2}{(2-s)^2}\left(R_s + \ R_h + \dfrac{R_d}{2-s}\right)^2 + \left(\left(R_s + R_h + \dfrac{R_d}{2-s}\right)^2 + (X_s + X_r)^2\right)\left(V_n^2 - \dfrac{(n_m\ V_n \cos\alpha)^2}{(2-s)^2}\right)}}{\left(R_s + R_h + \frac{R_d}{2-s}\right)^2 + (X_s + X_r)^2}. \tag{12}$$

$$T_p = \frac{3I_{rp}}{s\omega_s}(I_{rp}R_d - n_m V_p \cos\alpha), \tag{13}$$

$$T_n = \frac{3I_{rn}}{(2-s)\omega_s}(I_{rn}R_d - n_m V_n \cos\alpha), \tag{14}$$

$$T_e = \frac{3I_{rp}}{s\omega_s}(I_{rp}R_d - n_m V_p \cos\alpha) + -\frac{3I_{rn}}{(2-s)\omega_s}(I_{rn}R_d - n_m V_n \cos\alpha). \tag{15}$$

3. Stator Current Analysis of SPRIMDS under Unbalance Supply Voltage

IEC 60034-36 defines the voltage unbalance in terms of symmetrical sequence component equivalent to phase term as the ratio of negative sequence voltage component to positive sequence component, which is called true definition and is given by the following expression [24].

$$VUF\% = K_V = \frac{V_n}{V_p} \cdot 100. \tag{16}$$

A common definition of voltage unbalance is an extension of VUF, which is a Complex Voltage Unbalance Factor (CVUF) and is given in Eq. (17).

$$CVUF\% = \frac{V_n}{V_p} \cdot 100\angle\theta_v, \tag{17}$$

where θ_v is the angle of CVUF by which V_n leads the V_p, and this is a significant parameter for choosing the pattern of voltage under different voltage unbalance conditions. If V_a, V_b, and V_c are the phase voltage that are applied to the stator windings, hence the relation between unbalance phase voltage, positive sequence, and negative sequence voltage are given in Eq. (18) and Eq. (19), respectively.

$$V_p = \frac{V_a + aV_b + a^2V_c}{3} = V_p\angle\beta, \tag{18}$$

$$V_n = \frac{V_a + a^2V_b + aV_c}{3} = V_n\angle(\beta + \theta_v). \tag{19}$$

From Fig. 2, the positive and negative sequence currents can be written as in Eq. (20) and Eq. (21), respectively.

$$I_{sp} = \frac{V_p}{Z_p(\alpha)} = I_{sp}\angle(\beta - \phi_p), \tag{20}$$

$$I_{sn} = \frac{V_p}{Z_n(\alpha)} = I_{sn}\angle(\beta + \theta_v - \phi_n). \tag{21}$$

According to the symmetrical component analysis, unbalance phase current of the stator windings can be given by Eq. (22).

$$\begin{bmatrix} I_{sa} \\ I_{sb} \\ I_{sc} \end{bmatrix} = \begin{bmatrix} 1 & 1 \\ a^2 & a \\ a & a^2 \end{bmatrix} \begin{bmatrix} I_{sp} \\ I_{sn} \end{bmatrix}. \tag{22}$$

The stator Current Unbalance Factor ($CUFs$) [1], is given in Eq. (23).

$$CUFs = K_{C_s} = \left| \frac{I_{sn}}{I_{sp}} \right| = \frac{\frac{V_p}{Z_p}(\alpha)}{\frac{V_n}{Z_n}(\alpha)} = \frac{Z_p(\alpha)}{Z_n(\alpha)} K_V. \tag{23}$$

From Eq. (23) the K_{C_s} is directly proportional to K_V, and the ratio of $\frac{Z_p(\alpha)}{Z_n(\alpha)}$ is represents the sensitivity of K_{C_s} to K_V which is very high because Z_p is much higher than Z_n, since each of the positive and negative impedances is the function of the slip and firing angle (α). The Complex Current Unbalance Factor (CCUFs) of the stator current (CCUFs) can be given as in Eq. (24).

$$CCUFs = \frac{I_s n}{I_s p} = K_{C_s}(\alpha) \angle \theta_{cs} = \\ = \frac{Z_p(\alpha)}{Z_n(\alpha)} K_V \angle(\theta_v + \phi_p - \phi_n). \tag{24}$$

From Eq. (22), Eq. (23) and Eq. (24), the following expression of stator phase currents as a function of K_{C_s} and θ_{C_s} can be derived as in Eq. (25).

$$\begin{aligned} I_{sa} &= \mid I_{sp} \mid \sqrt{1 + K_{C_s}(\alpha)^2 + 2K_{C_s}(\alpha)\cos(\theta_{C_s})}, \\ I_{sb} &= \mid I_{sp} \mid \sqrt{1 + K_{C_s}(\alpha)^2 + 2K_{C_s}(\alpha)\cos(\theta_{C_s} - 120°)}, \\ I_{sc} &= \mid I_{sp} \mid \sqrt{1 + K_{C_s}(\alpha)^2 + 2K_{C_s}(\alpha)\cos(\theta_{C_s} + 120°)}. \end{aligned} \tag{25}$$

The limit and the range of variation of stator currents of SPRIMDS are given by Eq. (26) and Eq. (27), respectively.

$$I_{sp}(1 - K_{C_s}(\alpha)) \leq I_s \leq I_{sp}(1 + K_{C_s}\ (\alpha)), \tag{26}$$

$$\Delta I_s = I_{sp}(1 + K_{C_s}(\alpha)) - I_{sp}(1 - K_{C_s}\ (\alpha)) = \\ = 2K_V \frac{V_p}{V_n}. \tag{27}$$

4. Rotor Current Analysis under Unbalance Supply Voltage

The rotor complex current unbalance factor, CCUFr, is defined as in Eq. (28).

$$CCUF_r = \frac{I_{rn}}{I_{rp}} = K_{C_r} \angle \theta_{C_r}(\alpha). \tag{28}$$

From the positive and negative equivalent circuits of SPRIMDS, the expression of rotor phase currents as a function of K_{C_r} and θ_{C_r} can be derived as in Eq. (29).

$$\begin{aligned} I_{ra} &= \mid I_{rp} \mid \sqrt{1 + K_{C_r}(\alpha)^2 + 2K_{C_r}(\alpha)\cos(\theta_{C_s})}, \\ I_{rb} &= \mid I_{rp} \mid \sqrt{1 + K_{C_r}(\alpha)^2 + 2K_{C_r}(\alpha)\cos(\theta_{C_r} - 120°)}, \\ I_{rc} &= \mid I_{rp} \mid \sqrt{1 + K_{C_r}(\alpha)^2 + 2K_{C_r}(\alpha)\cos(\theta_{C_r} + 120°)}, \end{aligned} \tag{29}$$

where $\theta_{C_r}(\alpha) = \theta_v + \phi_p - \phi_n + \theta_2(\alpha) + \theta_1(\alpha) + 2n\pi/3$ and $n = 0, 1, 2$ is the minimum value of rotor current for phase a, b and c, respectively. Based on Eq. (9) and Eq. (10), $\theta_1(\alpha)$ and $\theta_2(\alpha)$ can be written as in Eq. (30) and Eq. (31), respectively.

$$\theta_1(\alpha) = 90° - \tan^{-1}\left(\frac{X_m + X_r}{R_h + \frac{R_d}{s}}\right), \tag{30}$$

$$\theta_2(\alpha) = 90° - \tan^{-1}\left(\frac{X_m + X_r}{R_h + \frac{R_d}{(2-s)}}\right). \tag{31}$$

The stator copper losses, the rotor copper losses, and developed torque can be re-written in terms $K_{C_s}(\alpha)$ and $K_{C_r}(\alpha)$ as in Eq. (32), Eq. (33) and Eq. (34), respectively.

$$P_{cu-loss}(\text{stator}) = 3I_{sp}^2(\alpha)R_s(1 + K_{C_s}^2(\alpha)), \tag{32}$$

$$P_{cu-loss}(\text{rotor}) = 3\frac{\pi^2}{9} I_{rp}^2(\alpha)R_d(1 + K_{C_r}^2(\alpha)), \tag{33}$$

$$T_e = \frac{3I_{rp}^2(\alpha)R_d}{\omega_s}\left(\frac{1}{s} - \frac{K_{C_r}^2(\alpha)}{2-s}\right) + \\ + \frac{3I_{rp}^2(\alpha)n_m V_p \cos(\alpha)}{\omega_s}\left(\frac{1}{s} - \frac{K_{C_r}(\alpha)}{2-s}\right). \tag{34}$$

5. Results and Discussions

Simulation of the proposed mathematical model has been carried out for analysing the performance of SPRIMDS model under different unbalance voltage conditions taking into consideration the effect of different firing angles. A typical WRIM of 1.8 kW, 380 V, 50 Hz, 4-pole has been used in the simulation. The parameters of the motor were measured in the electrical machine laboratory of Salahuddin University - Erbil. Parameters at the stator side are, $R_s = 2.4\ \Omega$, $X_s = 5.1\ \Omega$, $R_r = 3.42\ \Omega$, $X_r = 5.1\ \Omega$, and $X_m = 93.5\ \Omega$. SPRIMDS has been tested with unbalance supply voltage, in which the VUF varied from 0 % up to 10 %, to allow the motor performance state exceed the NEMA recommended range of 5 %. Furthermore, MATLAB Simulink is implanted to examine

Tab. 1: Input three-phase voltages, positive and negative sequence voltage components in terms of voltage unbalance factor applied to SPRIMDS.

VUF (%)	V_b (V)	V_c (V)	V_p (V)	V_n (V)
0	$220\angle -120°$	$220\angle 120°$	$220\angle 0°$	0
1	$217.9\angle -120.8°$	$216\angle 120°$	$218\angle -0.3°$	$3.2\angle 29.2°$
2	$216\angle -121.7°$	$212.3\angle 120°$	$216.1\angle -0.5°$	$4.4\angle 29.2°$
3	$214.4\angle -122.6°$	$208.5\angle 120°$	$214.2\angle -0.8°$	$6.5\angle 29.8°$
4	$212.8\angle -123.4°$	$204.7\angle 120°$	$212.5\angle -1.1°$	$8.5\angle 30°$
5	$211.3\angle -124.3°$	$201.5\angle 120°$	$210.7\angle -1.4°$	$10.5\angle 30°$
6	$209.7\angle -125.2°$	$197.8\angle 120°$	$209\angle -1.7°$	$12.7\angle 30°$
7	$208.1\angle -126°$	$194.3\angle 120°$	$207.1\angle -2°$	$14.6\angle 30°$
8	$207\angle -126.8°$	$191.3\angle 120°$	$205.7\angle -2.3°$	$16.5\angle 30°$
9	$205.7\angle -127.7°$	$188\angle 120°$	$204.1\angle -2.6°$	$18.4\angle 30°$
10	$204.5\angle -128.5°$	$184.6\angle 120°$	$202.5\angle -2.8°$	$20.3\angle 30°$

the behavior of SPRIMDS during the operation of unbalance supply voltage. The supply voltage of phase A has been adjusted to 220 V, and the other two-phase supply voltages B and C are adjusted to get the desired VUF percentage by varying the magnitude and phase angle as shown in Tab. 1.

5.1. Output Torque with Unbalance Factor for Different Firing Angles

To investigate the performance of SPRIMDS under unbalance conditions, torque-speed characteristics have been evaluated for $\alpha = 90°, 100°, 120°$, and $140°$. Figure 3 illustrates the variation of the developed electromagnetic torque with the rotor speed in different values of VUF $(0-10)$ % based on the proposed model. It has been seen that when the value of VUF % increases, the rotor speed, the starting torque, and the maximum torque reduce for different values of α. Also, Fig. 4 and Fig. 5 show comparisons of the proposed model and MATLAB simulation for ($\alpha = 100°$ and $120°$,), respectively. Results are found to be in good agreement for all values of VUF at different α. The average absolute error difference between the proposed model and simulation results at rated load is about 4 rpm.

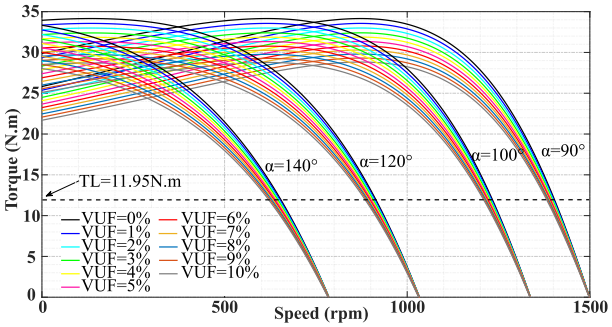

Fig. 3: Torque-speed characteristic of SPRIMDS for different VUF and firing angles.

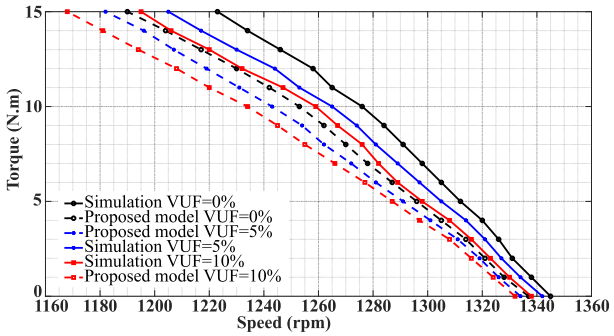

Fig. 4: Torque-speed characteristic of SPRIMDS for different values of VUF at $\alpha = 100°$ from the proposed model and simulation.

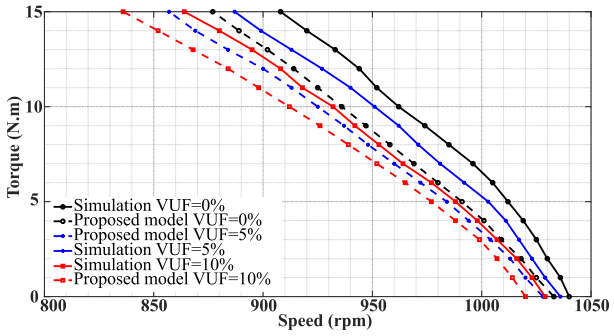

Fig. 5: Torque-speed characteristic of SPRIMDS for different values of VUF at $\alpha = 120°$ from the proposed model and simulation.

Table 2 shows the motor speed of the given drive system when is loaded by full load torque with various values of VUF within the given range, at $100°, 120°$ and $140°$, respectively. It is clear to see that the motor speed of the machine at constant load has reduced when VUF in supply is increased. It can be seen that the motor speed decreased from 1231 rpm to 1209 rpm, 914 rpm to 884 rpm and 654 rpm to 621 rpm, when VUF is increased from $(0-10)$ % for $\alpha = 100°, 120°$ and $140°$, respectively.

Table 3 shows the variation of starting torque and maximum torque with VUF, for different values of α.

The results obtained by the proposed model are verified by MATLAB simulation and the average absolute error is about 0.3 Nm. It can be noted that the maximum torque decreases from 34.15 to 28.82 Nm when VUF $(0-10)$ % increases, and it reduced by 15.6 % of its normal value at VUF = 10 %. The variation of starting torques with VUF $(0-10)$ % at different firing angles is observed in Tab. 3. The starting torque at $\alpha = 100°$ and $120°$ decreases from (29.92 to 25.14) Nm and (33.95 to 28.53) Nm, respectively. It is noted that the starting torque decreased by 15.97 % at a VUF of 10 %.

Tab. 2: The variation of rotor speed versus VUF % for different firing angles.

VUF (%)	Rotor speed (rpm) at full load torque		
	$\alpha = 100°$	$\alpha = 120°$	$\alpha = 140°$
0	1231	914	654
1	1230	911	651
2	1229	909	648
3	1225	906	645
4	1223	903	642
5	1222	900	639
6	1220	897	635
7	1217	894	632
8	1214	891	628
9	1212	888	624
10	1209	884	621

Tab. 3: The variation of the starting torque and maximum torque versus VUF for different firing angles.

VUF (%)	Starting torque (Nm)				Maximum torque (Nm)	
	$\alpha = 100°$		$\alpha = 120°$			
	Prop. model	Simu. model	Prop. model	Simu. model	Prop. model	Simu. model
0	29.92	30.24	33.95	34.27	34.15	34.45
1	29.4	29.75	33.36	33.67	33.56	33.87
2	28.91	29.35	32.8	33.12	32.99	33.31
3	28.37	28.68	32.2	32.65	32.4	32.7
4	27.92	28.25	31.67	32.01	31.88	32.21
5	27.43	27.72	31.13	31.46	31.34	31.65
6	26.93	27.27	30.56	30.87	30.79	31.10
7	26.49	26.81	30.06	30.41	30.29	30.61
8	26.03	26.35	29.55	29.86	29.8	3011
9	25.59	25.91	29.03	29.36	29.31	29.62
10	25.14	25.44	28.53	28.85	28.82	29.12

5.2. Influence of VUF on Motor Currents and Impedances

The positive sequence component, negative sequence component, and current unbalance factor of stator currents can be calculated based on Eq. (20), Eq. (21), and Eq. (23). The variation of the positive sequence current (I_{sp}), negative sequence current (I_{sn}), and (CUFs) as the result from the proposed model and MATLAB Simulation for ($\alpha = 100°, 120°$ and $140°$) versus VUF are shown in Fig. 6, Fig. 7 and Fig. 8, respectively. The CUF % of stator current increased from 0 % to 36 % when VUF is increased from 0 % to 10 % at $\alpha = 120°$. Also, the effect of firing angle α upon the I_{sp}, I_{sn}, and CUFs of the stator is shown in the same Figs. It can be observed that increasing α value from 100° to 140°, I_{sn} decreases from 1.85 A to 1.25 A, and I_{sp} decreases from 4.35 A to 3.85 A, while CUFs decreases from 43 % to 31 %.

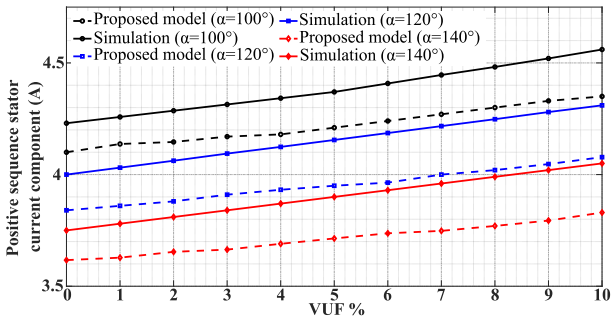

Fig. 6: Positive sequence component of stator current versus VUF for different values of α.

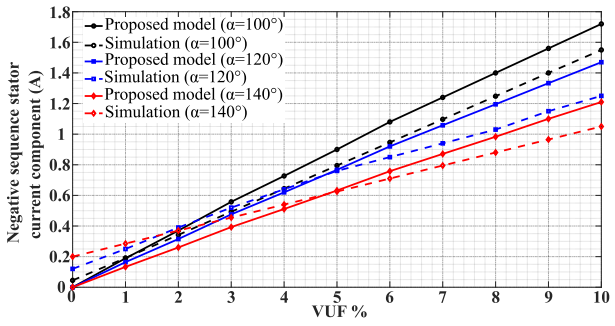

Fig. 7: Negative sequence component of stator current versus VUF for different values of α.

Figure 9 illustrates the variations of CUFs at slip values of 0.1, 0.2, and 0.33. It can be seen that CUFs increase linearly with VUF for a constant slip. At high speeds (low value of α), the CUFs is more sensitive to VUF, and at low speed (high value of α), the sensitivity becomes low. The ratio of VUF to CUF is equal to Z_p/Z_n, and both are the function of slip and α.

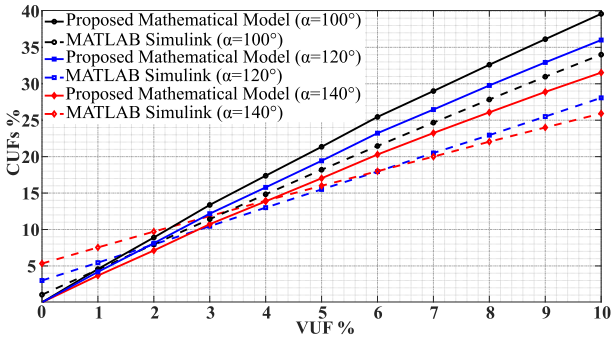

Fig. 8: *CUFs* versus VUF for different values of α.

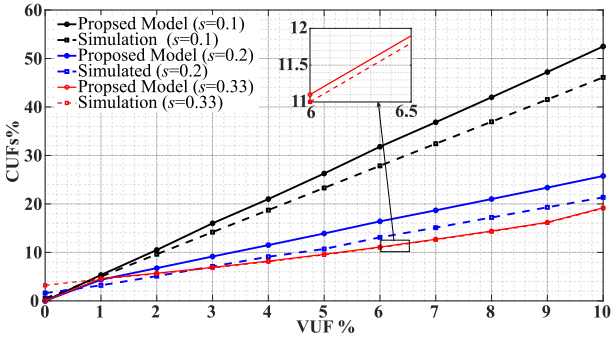

Fig. 9: $CUFs$ versus VUF for different values of slip.

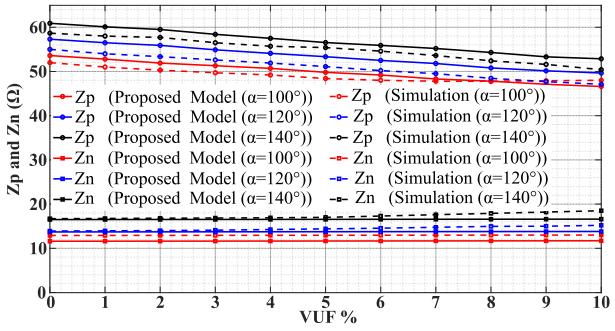

Fig. 10: The variation of positive and negative impedance versus VUF for different values of α.

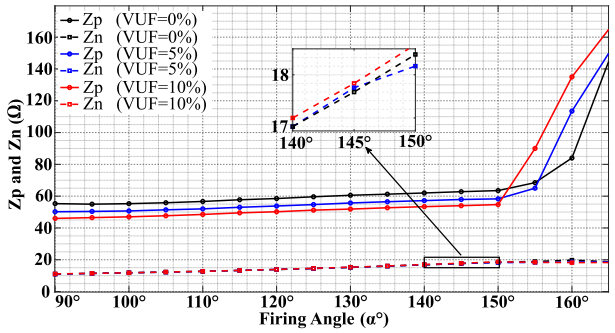

Fig. 11: The variation of positive and negative impedance versus α for different values of VUF.

Figure 10 shows the variation of Z_p and Z_n as a function of VUF % for different values of ($\alpha = 100°, 120°$ and 140°). It can be seen that Z_n increases and Z_p decreases with increasing VUF for different values of α. However, the rate of change of Z_p is higher than of Z_n.

Figure 11 shows the variation of Zp and Z_n based on Eq. (9) and Eq. (10) for firing angle inversion mode ($\alpha = 900$ to 1650) for VUF of 0 %, 5 % and 10 %. It can be observed that Z_n increases slightly with increasing α, while Z_p increases dramatically for high value of α due to the overlap angle of the inverter.

5.3. Influence of Voltage Unbalance Phase Angle on the Motor Currents at Constant VUF

Figure 12 shows the variation of the stator currents I_{sa}, I_{sb}, and I_{sc} versus θ_v which are obtained from Eq. (25), for VUF of 5 % (slip = 0.184), and VUF of 10 % (slip = 0.192), at full load torque and $\alpha = 100°$. It clearly can be noted that stator current significantly varies with θ_v in this range ($\Delta I_{\max} = 0.367$ A) for VUF of 5 %, and ($\Delta I_{\max} = 0.619$ A) for VUF of 10 %.

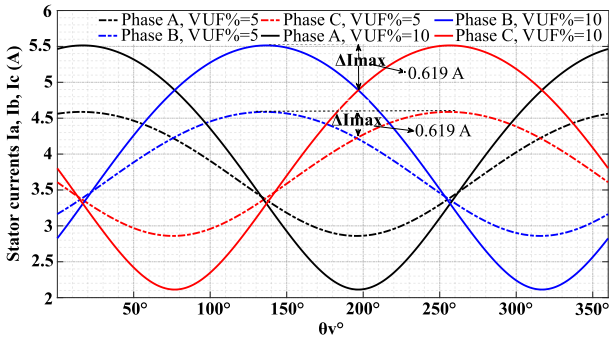

Fig. 12: The three-phase stator current versus θ_v for (VUF =5 % and 10 %) and $\alpha = 100°$.

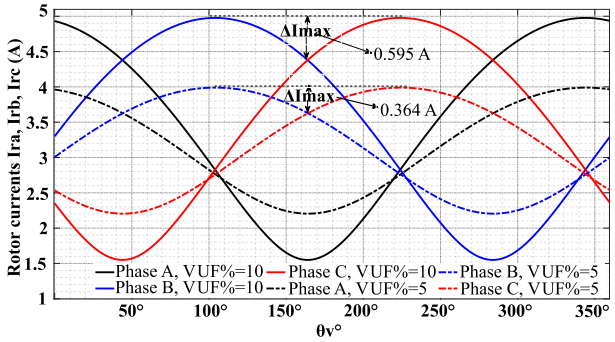

Fig. 13: The three-phase rotor current versus θ_v for (VUF =5 % and 10 %) and $\alpha = 100°$.

Figure 13 shows the variation of the rotor currents I_{ra}, I_{rb}, and I_{rc} against θ_v which are calculated from Eq. (29), for VUF of 5 % (slip = 0.184), and VUF of 10 % (slip = 0.192), at rated load and $\alpha = 100°$. It can be noticed that the rotor current significantly varies with θ_v in this range of ($\Delta I_{\max} = 0.364$ A) for VUF of 5 %, and ($\Delta I_{\max} = 0.595$ A) for VUF of 10 %.

5.4. Influence of VUF on the Power Factor and Efficiency

The variations of the power factors with VUF are shown in Fig. 14. It clearly can be seen that for $\alpha = 90°$, 100°, 120° and 140°, the power factor slightly

increases with increasing the VUF. Figure 15 shows the motor efficiency versus VUF for different values of α = 90°, 100°, 120° and 140°. The efficiency drops with increasing the asymmetry of the supply voltage. When the supply voltage is balanced for α = 90°, 100°, 120° and 140°, the efficiencies are 80.37 %, 77.9 %, 72.1 % and 63.8 %, while VUF becomes 10 %, the efficiencies are decreased to 74.5 %, 72 %, 64.5 % and 55.6 %, respectively, for the same α.

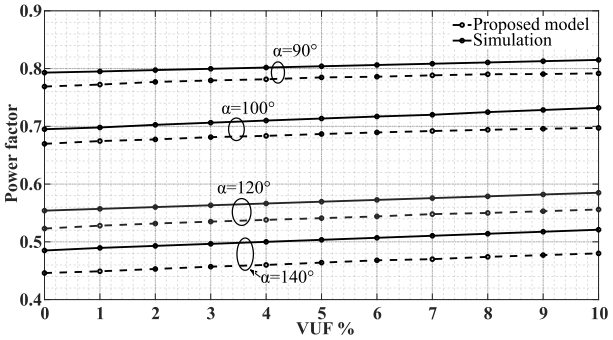

Fig. 14: The power factor versus VUF for different α.

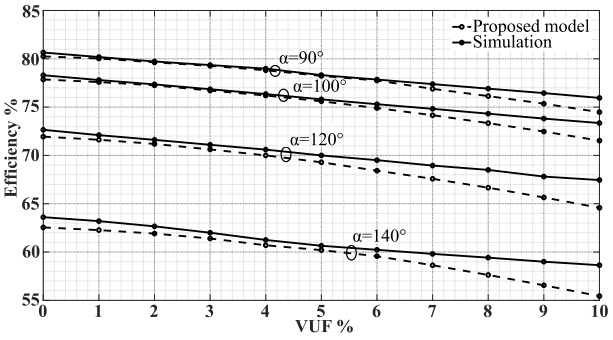

Fig. 15: The efficiency versus VUF for different α.

5.5. Influence of VUF on the Stator and Rotor Current Waveforms

Table 4 and Tab. 5 show the variation of THD of stator and rotor phase currents versus VUF, respectively. Noticeably, the THD increases significantly by increasing the degree of unbalanced supply. On the other hand, THD increases by increasing the firing angle of the inverter. However, the rotor current is more affected by increasing the VUF than the stator current.

Tab. 4: The variation of THD of stator and rotor currents for different values of VUF at $\alpha = 100°$.

VUF (%)	THD % of stator currents			THD % of rotor currents		
	I_{sa}	I_{sb}	I_{sc}	I_{ra}	I_{rb}	I_{rc}
0	2.24	2.69	2.32	7.07	6.91	7.11
1	2.91	2.76	2.79	8.35	8.16	8.19
2	4.04	3.85	3.86	10.15	9.98	10.12
3	5.12	5.29	5.35	12.81	12.7	12.33
4	6.17	6.76	6.92	15.26	14.86	15.13
5	7.12	8.16	8.49	17.81	17.37	17.81
6	8.18	9.86	10.25	20.54	20.37	20.17
7	9.05	11.2	11.63	23.02	22.89	23.33
8	9.66	12.22	12.65	25.33	25.74	25.22
9	10.22	13.37	13.4	28.75	28.29	27.52
10	10.54	14.27	14.31	30.76	31.85	30.26

Tab. 5: The variation of THD of stator and rotor currents for different values of VUF at $\alpha = 120°$.

VUF (%)	THD % of stator currents			THD % of rotor currents		
	I_{sa}	I_{sb}	I_{sc}	I_{ra}	I_{rb}	I_{rc}
0	5.55	5.31	5.61	15.14	15.29	15.18
1	5.61	5.41	5.72	15.25	15.61	15.48
2	5.88	5.58	5.95	16.12	16.05	15.96
3	6.26	5.98	6.45	17.73	17.37	17.36
4	6.44	6.1	6.66	18.65	18.27	18.59
5	7.18	6.3	7.25	20.31	20.95	20.34
6	7.83	6.7	7.95	22.89	21.98	22.15
7	8.23	7.45	8.55	24.22	23.45	23.45
8	8.71	7.96	8.93	25.5	26.06	25.87
9	9.29	8.5	9.7	26.5	26.8	26.57
10	9.66	9.2	10.13	27.81	28.51	27.96

6. Conclusion

In this paper, a mathematical model of SPRIMDS under the influence of unbalance supply voltage has been proposed. The proposed model was validated by using MATLAB/Simulink. The results for both mathematical model and simulation have shown that under unbalance supply conditions, the unbalance current depends on VUF, θ_v, positive and negative impedances, firing angle of the inverter, and the motor speed. However, there are some differences in mathematical models and simulation results due to different assumptions in derives of mathematical model and MATLAB/Simulink for reducing the complexity of the system. The results of this paper established that there are negative impacts of the unbalance supply on the performance of SPRIMDS.

Overall, the conclusion can be summarized as the following:

- Increasing the unbalance supply voltage at the rated load, the rotor speed is decreased for different firing angles.

- The sensitivity of current unbalance to voltage unbalance is given by the ratio of (Z_p/Z_n).
- At the constant value of VUF and speed, the maximum stator and rotor currents varied within a certain range according to the value of θ_v.
- The motor efficiency decreases with increasing the VUF, and the power factor increases with increasing the VUF due to decreasing the positive voltage component and hence decreasing the magnetizing currents.
- The maximum torque and starting torque decrease by increasing the VUF.
- For any value of VUF, the current unbalance factor decreased with increasing the inverter firing angle. Also, the CUF of stator current is high at high speed, and decreases with decreasing the motor speed.
- The THD of stator and rotor currents depends on the VUF, firing angle, and speed. Also, the rotor current is more sensitive to increasing the VUF than stator currents.

Author Contributions

H.F. has derived a mathematical model, performed the analytical calculations, and carried out the simulation. F.T. has contributed and supervised the overall work. Both H.F. and F.T. have provided critical comments, implemented the research, contributed to the interpretation and the writing of the final version of the manuscript.

References

[1] El-KHARASHI, E. and J. MASSOUAD. Approach to measure the degree of the unbalanced power in induction motor for energy-efficient use. *The Journal of Engineering*. 2017, vol. 2017, iss. 8, pp. 452–465. ISSN 2051-3305. DOI: 10.1049/joe.2017.0155.

[2] El-KHARASHI, E., J. MASSOUAD and M. Al-AHMAR. The impact of the unbalance in both the voltage and the frequency on the performance of single and cascaded induction motors. *Energy*. 2019, vol. 181, iss. 1, pp. 561–575. ISSN 0360-5442. DOI: 10.1016/j.energy.2019.05.169.

[3] QIU, H., Y. ZHANG, C. YANG and R. YI. The Influence of Stator–Rotor Slot Combination on Performance of High-Voltage Asynchronous Motor. *Journal of Control, Automation and Electrical Systems*. 2019, vol. 30, iss. 6, pp. 1126–1134. ISSN 2195-3899. DOI: 10.1007/s40313-019-00502-w.

[4] ADEKITAN, A. I. A New Definition of Voltage Unbalance Using Supply Phase Shift. *Journal of Control, Automation and Electrical Systems*. 2020. vol. 31, iss. 1, pp. 718–725. ISSN 2195-3899. DOI: 10.1007/s40313-020-00579-8.

[5] GANACINSKI, P., M. PEPLINSKI, D. HALLMANN and P. JANKOWSKI. Induction cage machine thermal transients under lowered voltage quality. *IET Electric Power Applications*. 2019, vol. 13, iss. 4, pp. 479–486. ISSN 1751-8660. DOI: 10.1049/iet-epa.2018.5242.

[6] AGAMLOH, E., A. CAVAGNINO and S. VASCHETTO. Standard efficiency determination of induction motors with a PWM inverter source. *IEEE Transactions on Industry Applications*. 2018, vol. 55, iss. 1, pp. 398–406. ISSN 1939-9367. DOI: 10.1109/TIA.2018.2869118.

[7] DONOLO, P. D., C. M. PEZZANI, G. R. BOSSIO, C. H. DE ANGELO and M. A. DONOLO. Derating of Induction Motors Due to Power Quality Issues Considering the Motor Efficiency Class. *IEEE Transactions on Industry Applications*. 2020, vol. 56, iss. 2, pp. 961–969. ISSN 1939-9367. DOI: 10.1109/TIA.2020.2965859.

[8] FAIZ, J. and H. EBRAHIMPOUR. Precise derating of three phase induction motors with unbalanced voltages. *Energy Conversion and Management*. 2007, vol. 48, iss. 9, pp. 2579–2586. ISSN 0196-8904. DOI: 10.1016/j.enconman.2007.03.023.

[9] FAIZ, J., H. EBRAHIMPOUR and P. PILLAY. Influence of unbalanced voltage on the steady-state performance of a three-phase squirrel-cage induction motor. *IEEE Transactions on Energy Conversion*. 2004, vol. 19, iss. 4, pp. 657–662. ISSN 1558-0059. DOI: 10.1109/TEC.2004.837283.

[10] EL-KHARASHI, E., M. EL-DESSOUKI, J. G. MASSOUD, A. W. FARID and M. A. AL-AHMAR. The use of the current complex factor to determine the precise output energy of the induction motor. *Electric Power Systems Research*. 2018, vol. 154, iss. 1, pp. 23–36. ISSN 0378-7796. DOI: 10.1016/j.epsr.2017.08.008.

[11] VON JOUANNE, A. and B. BANERJEE. Assessment of voltage unbalance. *IEEE Transactions on Power Delivery*. 2001, vol. 16, iss. 4, pp. 782–790. ISSN 1937-4208. DOI: 10.1109/61.956770.

[12] ABDELFATTAH, M. Y. and M. M. AHMED. An artificial neural network-based chopper-controlled slip-ring induction motor. In: *11th IEEE Mediterranean Electrotechnical Conference*. Cario: IEEE, 2002, pp. 142–146. ISBN 0-7803-7527-0. DOI: 10.1109/MELECON.2002.1014547.

[13] RAM, S., O. P. RAHI, V. SHARMA and K. S. R. MURTHY. Investigations in to Induction Motor Drive using Slip Power Recovery Scheme with GTO Inverter and Chopper. In: *2017 14th IEEE India Council International Conference (INDICON)*. Roorkee: IEEE, 2017, pp. 1–6. ISBN 978-1-5386-4318-1. DOI: 10.1109/INDICON.2017.8487590.

[14] BHARDWAJ, S. R., O. P. RAHI and V. SHARMA. Comparative Analysis of Induction Motor Drive with Chopper Controlled SPRS Employing Various Inverter Configurations. *IETE Journal of Research*. 2019, vol. 65, iss. 3, pp. 329–341. ISSN 0974-780X. DOI: 10.1080/03772063.2018.1431065.

[15] BANGARRAJU, J., V. RAJAGOPAL and A. J. LAXMI. Power quality enhancement using power balance theory based DSTATCOM. *Advances in Electrical and Electronic Engineering*. 2016, vol. 14, iss. 1. pp. 1–10. ISSN 1804-3119. DOI: 10.15598/aeee.v14i1.1342.

[16] TUNYASRIRUT, S. and V. KINNARES. Speed and power control of a slip energy recovery drive using voltage-source PWM converter with current controlled technique. *Energy Procedia*. 2013, vol. 34, iss. 1, pp. 326–340. ISSN 1876-6102. DOI: 10.1016/j.egypro.2013.06.761.

[17] DATTA, R. and V. RANGANATHAN. Rotor side control of grid-connected wound rotor induction machine. *Journal of the Indian Institute of Science*. 2013, vol. 80, no. 5, pp. 437–456. ISSN 0970-4140.

[18] BHARDWAJ, S. R., O. P. RAHI and V. SHARMA. Performance analysis of SPRS-based induction motor drive using multi-level inverter and buck-boost chopper. *International Journal of Power Electronics*. 2020, vol. 12, no. 1, pp. 85–100. ISSN 1756-6398. DOI: 10.1504/IJPELEC.2020.108387.

[19] CADIRCI, I., G. AKCAM and M. ERMIS. Effects of instantaneous power-supply failure on the operation of slip-energy recovery drives. *IEEE Transactions on Energy Conversion*. 2005, vol. 20, iss. 1, pp. 7–15. ISSN 1558-0059. DOI: 10.1109/TEC.2004.837303.

[20] DAVIES, S. Q. and J. M. VAN COLLER. Investigating the vulnerability of slip energy recovery converters to voltage dips. In: *Conference Record of the 2006 IEEE Industry Applications Conference Forty-First IAS Annual Meeting*. Tampa: IEEE, 2006, pp. 1702–1708. ISBN 1-4244-0364-2. DOI: 10.1109/IAS.2006.256765.

[21] LAZRAK, A. and A. ABBOU. H∞ Control of Wrim Driven Flywheel Storage System to Ride-Through Grid Voltage Dips. *Advances in Electrical and Electronic Engineering*. 2020, vol. 18, iss. 1. pp. 11–22. ISSN 1804-3119. DOI: 10.15598/aeee.v18i1.3546.

[22] WANG, Y. J. Analysis of effects of three-phase voltage unbalance on induction motors with emphasis on the angle of the complex voltage unbalance factor. *IEEE Transactions on Energy Conversion*. 2001, vol. 16, iss. 3, pp. 270–275. ISSN 1558-0059. DOI: 10.1109/60.937207.

[23] LEE, C.-Y., B.-K. CHEN, W.-J. LEE and Y.-F. HSU. Effects of various unbalanced voltages on the operation performance of an induction motor under the same voltage unbalance factor condition. *Electric Power Systems Research*. 1998, vol. 47, iss. 3, pp. 153–163. ISSN 0378-7796. DOI: 10.1016/S0378-7796(98)00035-2.

[24] IEC 60034-26:2006. Rotating electrical machines - Part 26: Effects of unbalanced voltages on the performance of three-phase cage induction motors. Geneva: IEC Standard. 2006.

About Authors

Hilmi Fadhil AMEEN was born in Sulaymaniyah-Iraq. He received his M.Sc. from University of Technology, Baghdad - Iraq in 2003. He is currently Assist. Prof. at Department of Electrical Engineering at Salahaddin University-Erbil, Iraq. His research interests include electrical machine drive system and electrical power quality.

Fadhil Toufick AULA was born in 1970 in Erbil, Kurdistan Region, Iraq. He received his M.Sc. in Electrical Engineering from the College of Engineering at Salahaddin University-Erbil, Iraq in 2002, and Ph.D. degree in the College of Engineering, School of Electrical and Computer Engineering at the University of Oklahoma, Norman, USA in 2013. He is currently assist. Prof. and head of the Department of Electrical Engineering at Salahaddin University-Erbil. His topic of research focuses on automation systems, control engineering, renewable power system, and power system analysis.